

High directivity microstrip antenna with stopband and passband frequency selective surfaces for 6G at low-THz

Uri Nissanov, Ghanshyam Singh

Department of Electrical and Electronic Engineering Science, Auckland Park Kingsway Campus, University of Johannesburg, Johannesburg, South Africa

Article Info

Article history:

Received April 29, 2021

Revised Jun 9, 2022

Accepted Jul 5, 2022

Keywords:

6G

Ansys high-frequency structure simulator

Computer simulation

technology microwave studio

Low-THz antennas

ABSTRACT

There is still no high-directivity microstrip antenna with directivity beyond 25 dBi, bandwidth (BW) of more than 24%, which can be used for 6G cellular communication at low-THz at a resonance frequency of 144 GHz. So, duo broadband microstrip antennas have been designed at a resonance frequency of 144 GHz with the Taconic TLY-5 laminate in this work. These designs were carried out with the computer simulation technology microwave studio (CST MWS) software. The first antenna simulation results were compared within an Ansys high-frequency structure simulator (HFSS) software, and the obtained simulation results from both software were in fair consent, supporting the proposed designs. The peak directivity, peak gain, total peak efficiency, and BW obtained for the proposed THz microstrip antennas were 27.01 dBi, 25.3 dB, 78.96%, and 34.21 GHz (24.93%), respectively. Therefore, these antennas can be a base for 6G at low-THz.

This is an open access article under the [CC BY-SA](https://creativecommons.org/licenses/by-sa/4.0/) license.



Corresponding Author:

Uri Nissanov

Department of Electrical and Electronic Engineering Science

Auckland Park Kingsway Campus, University of Johannesburg, Johannesburg 2006, South Africa

Email: uri1636@gmail.com

1. INTRODUCTION

The terahertz (THz) band is a frequency spectrum from 100-10,000 GHz and is located between the optical regimes and millimeter wave (mmWave). Because of researchers' lack of development in technologies of efficient detectors, low-loss connectors, high-gain antennas, and high-power sources in solid-state technology, this frequency band has been defined as the "THz bandgap" [1]–[5]. Last year's development of ultra-fast cellular mobile communication systems increases THz technologies and THz antennas' demand to increase data transmission at a high data rate of tens of Gb/s, even to Tb/s, so we must use the THz band. The THz band offers a wide bandwidth (BW) that is not used. The THz waves experience meaningful absorption per oxygen molecules and atmospheric water vapor, and because of that, we must work at frequency window bands, where the humid atmosphere loss is below 0.1 dB/m. At frequencies below 1 THz, these windows exist around 0.125–0.175 THz and 0.2–0.3 THz [1]–[5]. According to [6], the authors determined that the minimal antenna gains at these THz antennas need 20 dB. Therefore, the THz antenna needs a BW of a minimal 4.1 GHz to facilitate a data rate of 20 Gb/s.

According to [7], the authors modeled, optimized, and simulated with an Ansys high-frequency structure solver (HFSS), duo 1 THz antennas, with metamaterials for increasing the antenna's gain. The first was a microstrip antenna, and the second was a bow-tie patch antenna. The peak gain and BW obtained were 8.82 dB, 16 GHz (1.6 %), 12.92 dB, and 50 GHz (5%). According to [8], the authors modeled, optimized, and simulated with the Ansys HFSS software four 272 GHz microstrip antennas models. These antennas included benzo cyclobutene (BCB) substrate, gallium nitride (GaN) substrate, and low resistive silicon

(LR Si) substrate. The peak directivity, peak gain, peak radiation efficiency and BW obtained to 1st–4th models were 7.5 dBi, 1.6 dB, 24%, 10 GHz (3.67%), 7.8 dBi, 2.4 dB, 29%, 7 GHz (2.57%), 8.1 dBi, 2.5 dB, 30%, 8 GHz (2.94%), 8.3 dBi, 3.4 dB 32%, 11 GHz (4%), respectively. According to [9], the authors modeled, optimized, and simulated with the computer simulation technology microwave studio (CST MWS) software a dielectric lens antenna at 270 GHz. The antenna consists of an expanded hemispherical lens with a WR-3 rectangular waveguide input. A prototype THz antenna has been manufactured using computer numerical control (CNC) milling and experimentally validated to verify the simulation results. The proposed antenna's peak measured gain was approximately 30 dB, with a BW of 80 GHz (30%). According to [10], the authors modeled, optimized, and simulated a 1,000 GHz directional 1×2 array antenna with an Ansys HFSS software. The antenna contained a three-layer structure of the top copper, BCB dielectric laminate, and bottom copper. The peak gain and BW attained were 5.87 dBi, and 210 GHz (21.3%). Faridani and Khatir [11] modeled, optimized, and simulated an 800 GHz wideband antenna with a Quartz hemisphere lens and microstrip patch antenna based on Rogers RT5880LZ substrate. The BW, peak gain, and radiation efficiency attained were 800 GHz (100%), 13.2 dB, and 95%. Out of the reported published works [7]–[11], it can have been shown that there is still no high-directivity microstrip antenna with directivity beyond 25 dBi, and BW of more than 24%, which can be used for 6G cellular communication at low-THz at the resonance frequency of 144 GHz.

This research investigates a low-THz antenna's design and simulation at a resonance frequency of 144 GHz, with good directivity and BW to establish a communication propagation range of over 100 m and enable a data rate of 20 Gb/s for 6G. This research paper is ship-shaped as follows. Clause 1 presents the introduction and the relevant works. While clause 2 presents the research method. Clause 3 presents the results and discussion. Moreover, in the end, clause 4 concludes this work.

This paper's innovation was to model microstrip antennas with a peak directivity of more than 25 dBi, BW of more than 20%, at the low-THz band for 6G @144 GHz. These antennas included a Taconic TLY-5 microstrip laminate, and one antenna model included stopband frequency selective surfaces (FSSs) and passband FSSs. This design was compared with an Ansys HFSS software.

2. RESEARCH METHOD

An empirical evaluation with manufacturing a prototype low-THz antenna needful be used to verify the offered antenna's simulation results. However, software equalizations were chosen for this research to reduce this verification's high price and reach beyond a couple of thousand Euros. Therefore, it is optimal to use dual different commercial electromagnetic (EM) software, which works at different methods, to obtain a decent simulation equalization that the simulation results will be similar to each other, which has also been used at [12], [13].

The third dimension (3D) commercial EM CST MWS software includes some diverse solvers [14], where every solver works with other methods. In this work, the design and simulation were with the time-domain solver in the CST MWS software based on the finite-difference-time-domain (FDTD). This simulation with the CST MWS software was done with adaptive mesh hexahedral type, and –40 dB accuracy was defined, and boundary conditions as an open condition at the X, Y, and Z-axis were applied.

The first proposed antenna was also simulated with the commercial 3D EM finite element (FEM) solver at the Ansys HFSS 17.2 solver [15] for comparison and to diminish the high price of empirical evaluation [12], [13]. At the Ansys HFSS software, the adaptive mesh at auto mode was defined with the peak number of passes of 30 and peak delta S of 0.02, while the solution options were defined as first order with direct solver, and the frequency sweep type was defined as fast, and the virtual radiation boundary with vacuum was chosen to at least $\lambda_0/4$ away from the antenna.

This paper modeled and simulated a couple of THz microstrip array antennas with 26×32 slotting radiators at parallel and series-fed for a frequency of 144 GHz. The first was modeled at a single printed circuit board (PCB) and excluded stopband and passband FSSs, while the second included stopband and passband FSSs beside the slotting radiators.

2.1. The structure of the first proposed THz antenna

This first antenna was made with a Taconic TLY-5 microstrip laminate within the parameters of copper thickness (t), substrate height (h), loss tangent ($\tan\delta$) and dielectric constant (ϵ_r): 17.5 μm , 127 μm , 0.0009 μm , 2.2 μm , respectively. The ϵ_r of a Taconic TLY-5 substrate is 2.253 ± 0.001 @ (0.325 – 0.5) THz, while the loss tangent is $9.43 \cdot 10^{-3} - 1.11 \cdot 10^{-2}$ @ (0.325 – 0.5) THz [16]. Choosing the right microstrip laminate becomes a critical challenge at Sub-mm and mm wavelengths due to the laminate losses and conductor losses [14]–[16]. All printed circuit boards (PCBs) have conduction losses and dielectric losses. And hence with these laminate parameters, which were ($h = 127 \mu\text{m} \leq \lambda_{\text{high}}/8 = 242 \mu\text{m}$),

($t = 17.5 \mu\text{m} \leq \lambda_{\text{high}}/8 = 242 \mu\text{m}$, $\epsilon_r = 2.2 < 3.5$, $\tan(\delta) = 0.0009 < 0.0095$) [17]–[19], the above effects were reduced to a minimum. This substrate was built with a Wilkinson 1×32 divider and 26×32 slotting radiators.

The sizes of the substrate were $47 \times 55 \text{ mm}^2$, which equals $22.5\lambda_0 \times 26.4\lambda_0 @ 144 \text{ GHz}$. Serial array antennas can be graded as traveling-wave antennas or resonant antennas [20]. A combination of parallel and series-fed techniques must be used to avoid the main beam squint as frequency changes. So, in this research paper, parallel and series fed together have been used. Figure 1 presents the designed microstrip array antenna for 144 GHz, while Figure 1(a) shows the principal structure of slotting patch radiators, and Figure 1(b) shows the completely designed first THz antenna. After optimizing with the CST MWS software, the following optimized antenna dimensions were received and uploaded in Table 1.

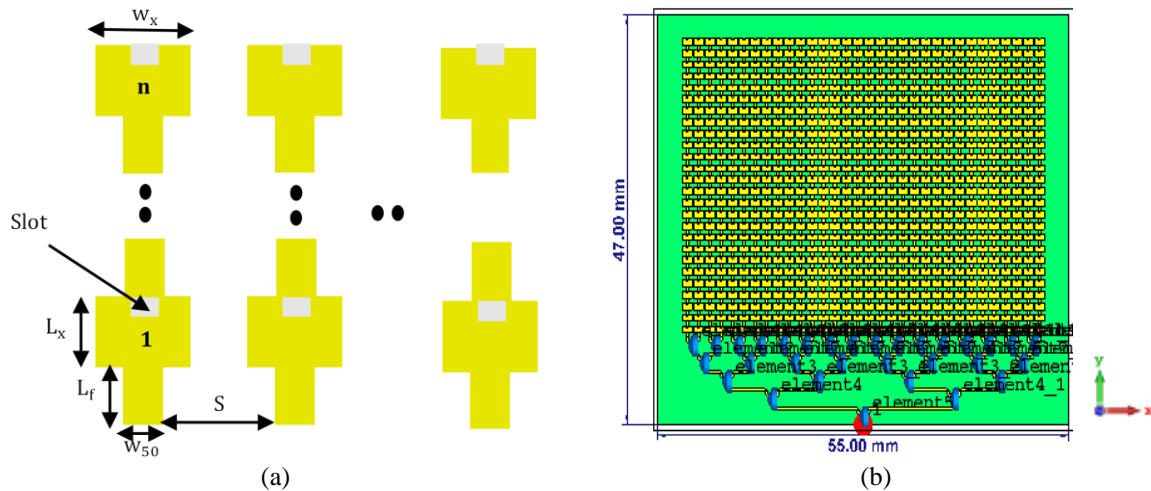


Figure 1. Structure of the first THz antenna without FSS (a) principal structure of the slotting patch radiation elements and (b) the complete antenna

Table 1. The optimized dimensions of the antennas

Parameter	Size at antennas
S	1153 μm
W_x	1383 μm
L_x	1780 μm
W_{50}	370 μm
Slotting sizes	$200 \times 200 \mu\text{m}^2$

2.2. The formation of the microstrip antenna, including passband and stopband FSSs

According to [21], FSSs are 2D periodic human-made structures modeled to present EM features that cannot be accomplished from natural structures. FSS is materialized by printing sub-wavelength copper cells periodically on a laminate and placed under a layer above the radiators when used in antennas. Figure 2 shows the formation of the microstrip antenna combined with a passband and stopband FSSs.

The upper substrate (superstrate) included passband FSSs to reduce the surface waves and substrate losses. The lower substrate included stopband FSSs, as a ground plane, to reflect the plane wave in-phase. The gaps between the microstrip array and the FSS substrates were an air gap, and h_1 was the air-gap distance. After the optimization is done with the CST MWS software, the h_1 was set to: $h_1 = 0.874 \text{ mm} = 0.4\lambda_0 @ 130 \text{ GHz}$, to get a maximum boost to second THz antenna gain.

2.3. The unit-cell modeled stopband FSS and unit-cell modeled passband FSS structures

The modeled stopband FSS was done with a printed copper ring with a rectangular line on a Taconic TLY-5 microstrip laminate with the sizes of $1000 \times 1000 \mu\text{m}$, which equal to $0.433\lambda_0 \times 0.433\lambda_0 @ 130 \text{ GHz}$. Figure 3(a) shows the unit-cell modeled stopband FSS structure for 130 GHz, while Figure 3(b) shows the unit-cell modeled passband FSS for 130 GHz, and it is in a complementary structure to the unit-cell modeled stopband FSS. After optimization with the CST MWS software, the sizes of the unit-cell FSS were set to: $W_1 = 1 \text{ mm}$, $W_2 = 0.12 \text{ mm}$, $X_1 = 0.9 \text{ mm}$, $X_2 = 0.66 \text{ mm}$, $X_3 = 0.05 \text{ mm}$.

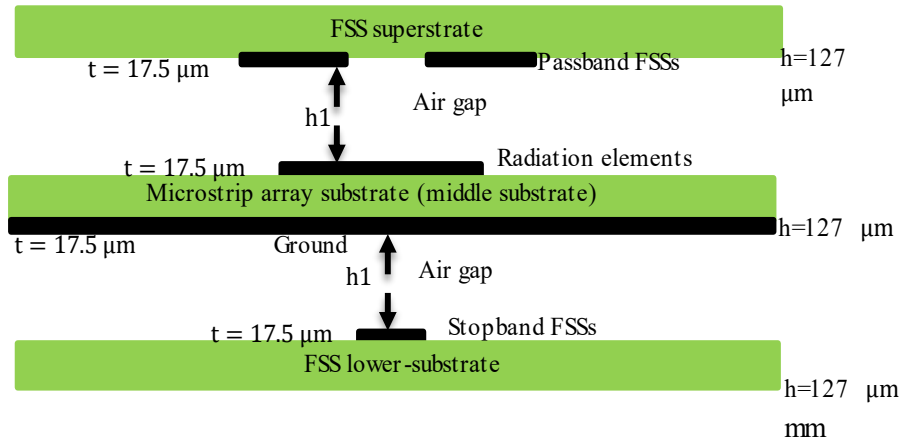


Figure 2. The formation of a microstrip antenna including passband and stopband FSSs

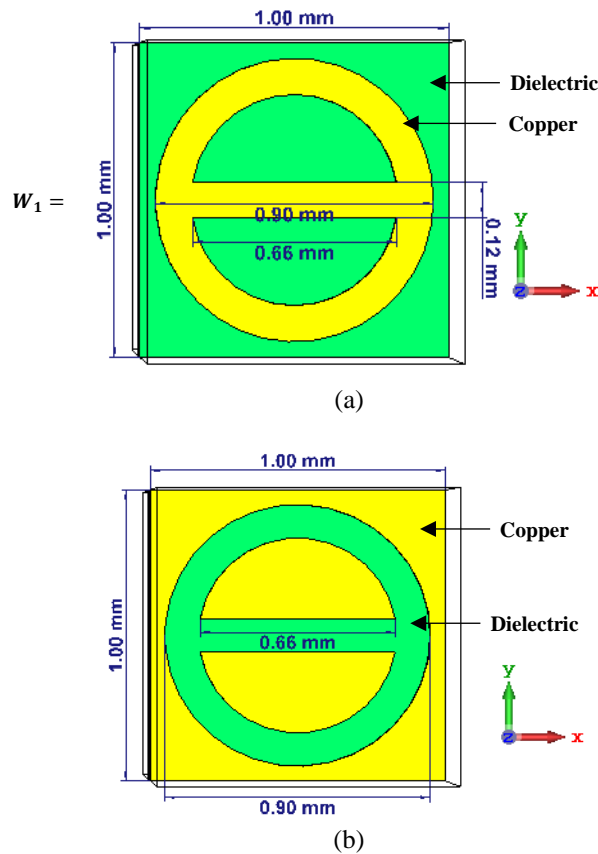


Figure 3. The FSSs structure (a) the unit-cell modeled stopband FSS and (b) the unit-cell modeled passband FSS structure

2.4. The second proposed THz antenna structure

The second THz antenna was designed and simulated at three PCBs with FSS superstrate and 25 stopbands FSSs, FSS lower substrate with 25 passband FSSs, Wilkinson 1x32 divider, and 26x32 slotting patch radiators at the middle substrate. All PCBs were made with the Taconic TLY-5 microstrip laminate with the same parameters as the first THz antenna. Figure 4 shows the modeled second THz antenna with FSSs, while Figure 4(a) shows the side vies of the complete microstrip antenna, Figure 4(b) shows the antenna array at the middle substrate, and Figures 4(c) and 4(d) shows the part of passband FSSs superstrate and stopband FSSs in the lower substrate, respectively.

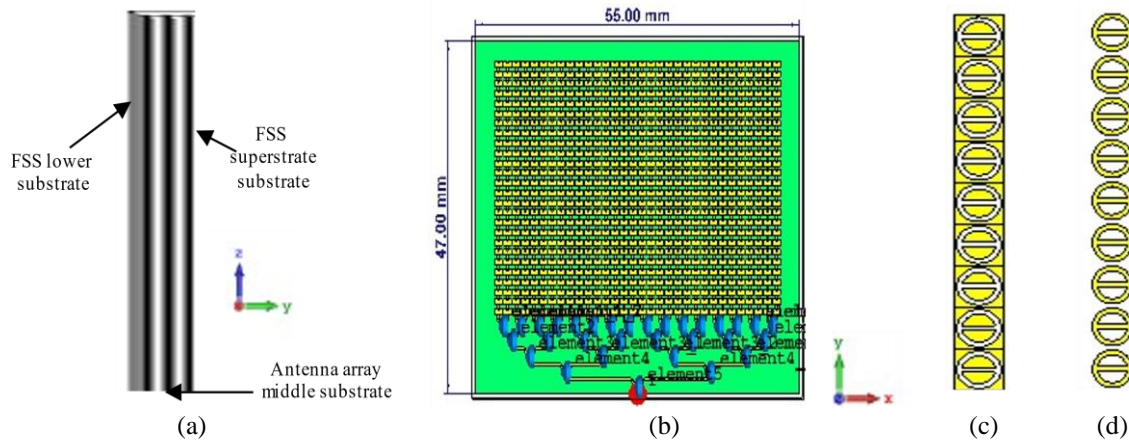


Figure 4. The second THz antenna with FSSs, (a) side view of complete microstrip array, (b) antenna array middle substrate, (c) part of FSS superstrate, and (d) part of FSS lower-substrate

2.5. Computation of the BW and gain of the suggested low-THz antennas

Following [1], [3], and [22]–[28], and for the resonance frequency of 144 GHz, the lowest level BW and antenna gain is 4.1 GHz, 16.85 dB, a base for a 6G cellular communication antenna. So, the design goal of our THz antenna with a minimum gain was 24 dB, while the minimum impedance BW was 24%. A parallel and series-fed together microstrip array antenna has been used to attain this minimum gain, while a slotting patch has been used to attain this minimum impedance BW.

3. RESULTS AND DISCUSSION

3.1. Simulation results of the first proposed low-THz antenna

The simulated S_{11} result of the first proposed THz antenna is shown in Figure 5. From Figure 5, it has been shown that the BW ($S_{11} \leq -10$ dB) of this antenna is: 34.39 GHz (25.04%), while the resonance frequency is 144 GHz and the minimum S_{11} is equal to -50.6 dB. Figures 6(a) and 6(b) shows the 2D simulation result of the gain, and the 3D simulation result of the directivity @126 GHz of this antenna, respectively.

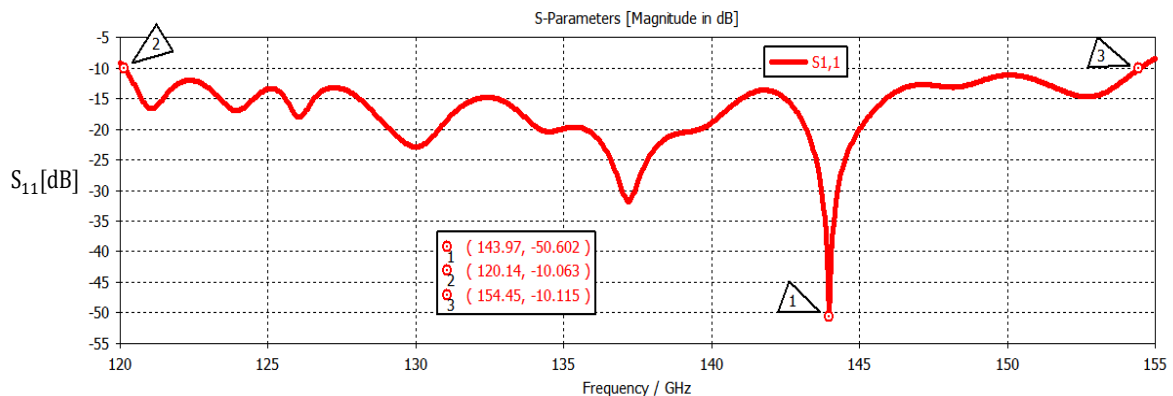


Figure 5. Simulation result of the return loss (S_{11}) for the first proposed low-THz antenna

From Figure 6(a), it has been shown that the gain was between 6.87 – 24.73 dB at the frequency range of 120–135 GHz. From Figure 6(b), it has been shown that the maximum directivity was found as 25.59 dBi@126 GHz. The radiation and the total efficiency simulated results of this antenna are shown in Figure 7. From Figure 7, it has been shown that radiation efficiency was between 75.5% – 81.8%, while the total efficiency was between 66.53% – 80.99% at 120–135 GHz.

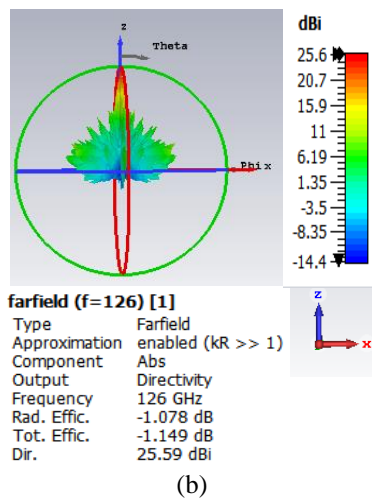
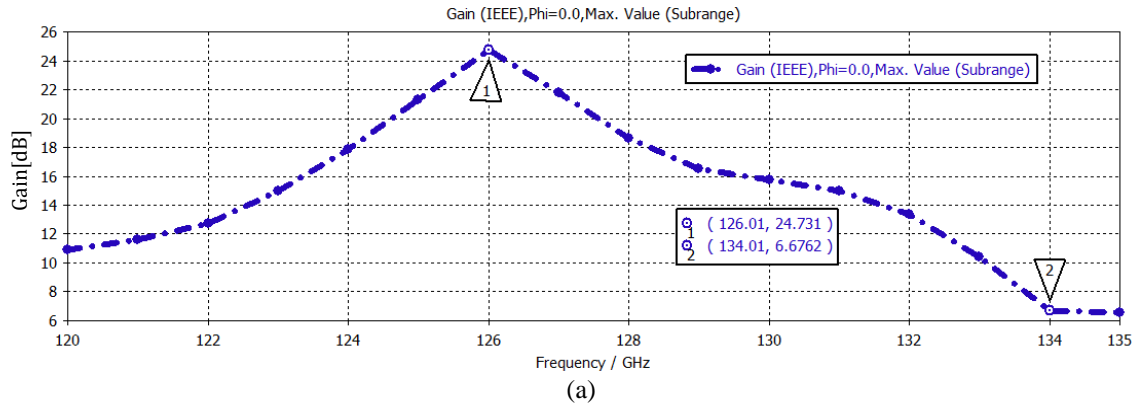


Figure 6. The gain and the directivity simulation result for the first proposed low-THz antenna (a) gain and (b) directivity

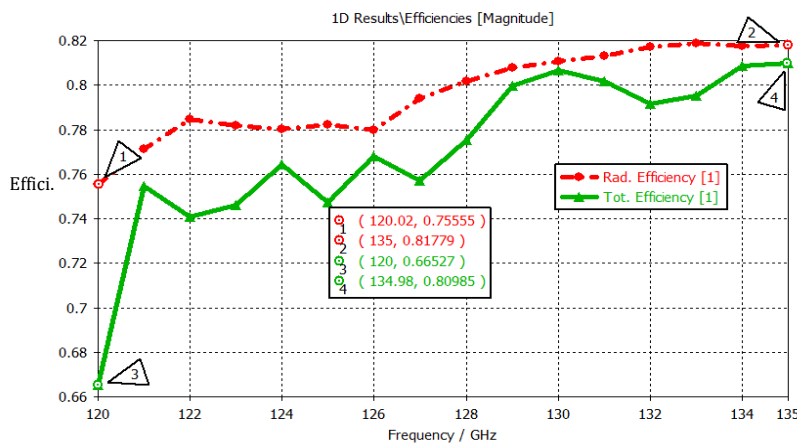


Figure 7. The radiation and the total efficiency simulated results of the first proposed low-THz antenna

3.2. The unit-cell modeled stopband FSS and passband FSS simulated results

The simulated S-parameters of the modeled unit-cell stopband are shown in Figure 8. From Figure 8, it has been shown that the $S_{11} \leq -10$ dB for 104.1–153.4 GHz, while the $S_{21} < -0.48$ dB for 104.1–153.4 GHz. The simulated S-parameters of the modeled unit-cell passband FSS are shown in Figure 9. From Figure 9, it has been shown that the $S_{11} \leq -10$ dB for 131.91–175.2 GHz, while the $S_{21} < -0.47$ dB for 131.91–175.2 GHz.

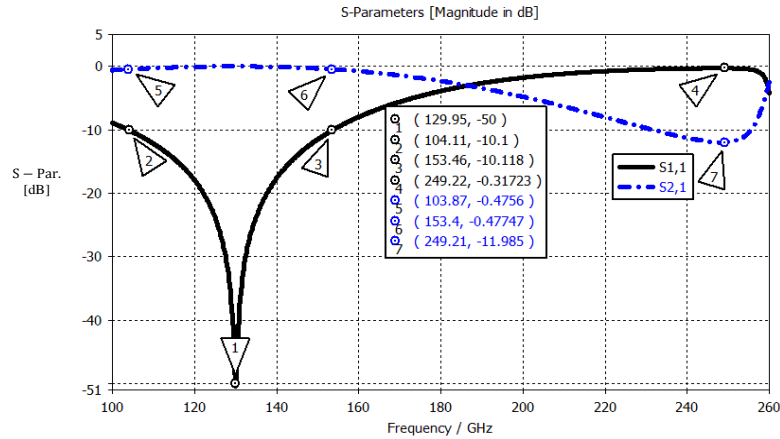


Figure 8. The transmission coefficient (S_{21}) and reflection coefficient (S_{11}) simulated results of the unit-cell modeled stopband FSS

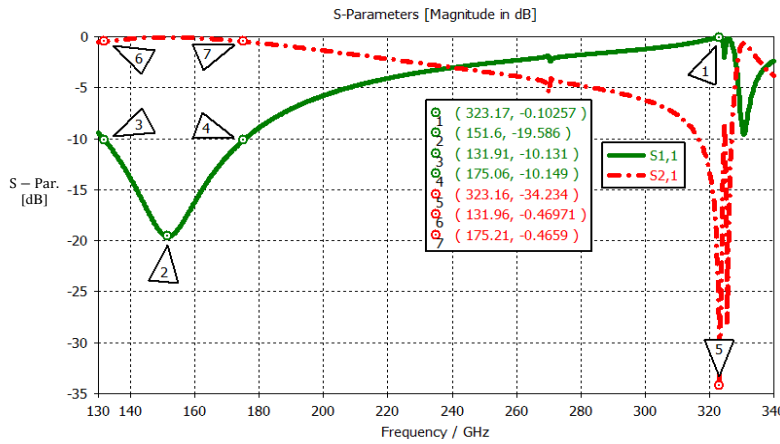


Figure 9. The S_{21} and the S_{11} simulated results of the modeled unit-cell passband FSS

3.3. The second proposed low-THz antenna simulation results

The simulated S_{11} result of the second proposed THz antenna is shown in Figure 10. From Figure 10, it has been shown that the BW($S_{11} \leq -10$ dB) of this antenna is 34.21 GHz (24.93%), while the resonance frequency is 143.7 GHz and the minimum S_{11} is equal to -40 dB. Figures 11(a) and 11(b) shows the 2D simulation result of the gain, and the 3D simulation result of the directivity @126 GHz of this antenna, respectively.

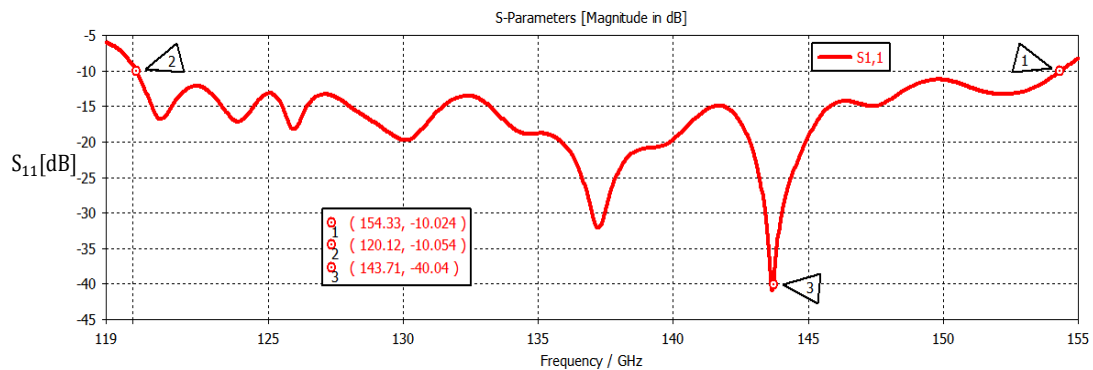


Figure 10. The S_{11} simulation result of the second proposed low-THz antenna

From Figure 11(a), it has been shown that the gain was between 5.73 – 25.3 dB at 120–135 GHz. From Figure 11(b), it has been shown that the maximum directivity was found as 27.01 dBi@126 GHz. The simulated radiation and the total efficiency results of this antenna are shown in Figure 12. From Figure 12, it has been shown that radiation efficiency was between 74.17% – 80%, while the total efficiency was between 65.32% – 78.96% at 120–135 GHz.

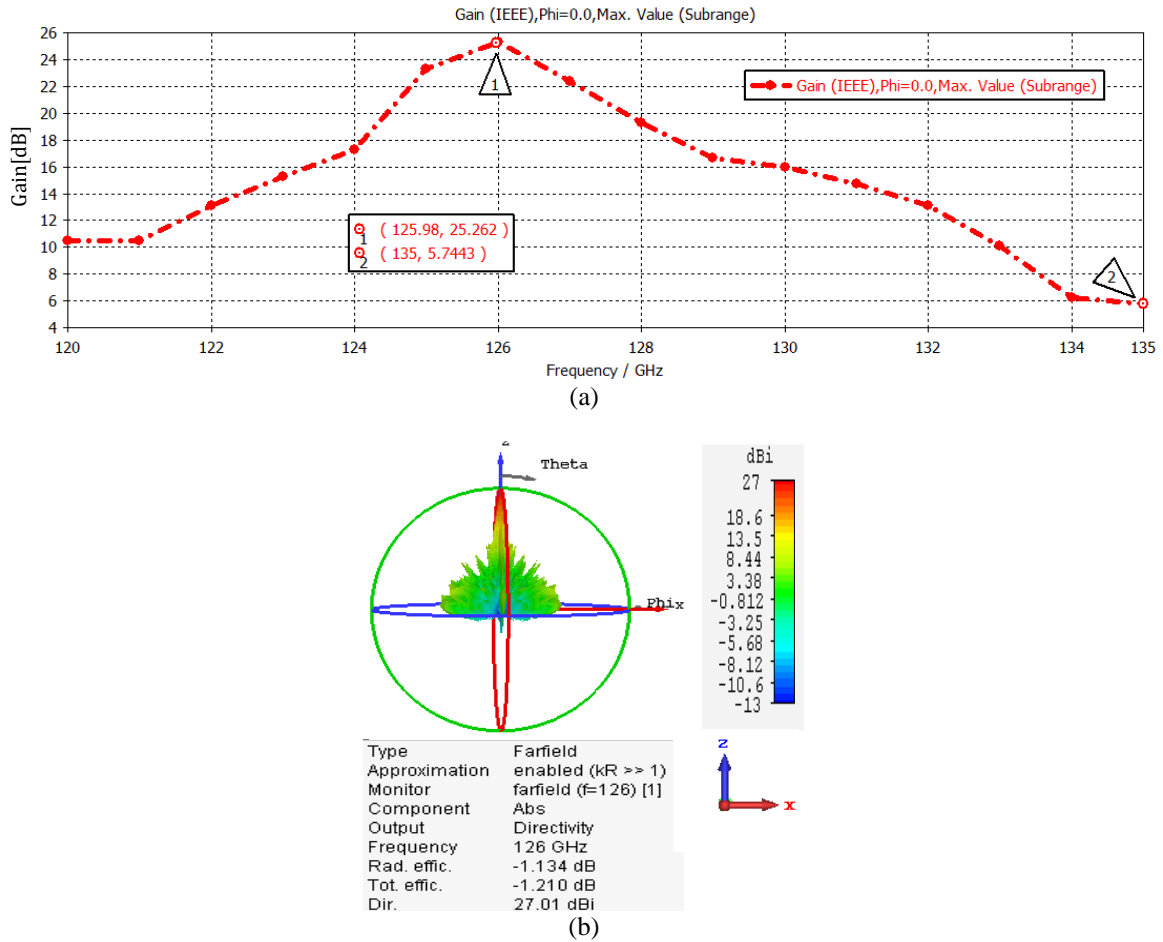


Figure 11. The directivity and the gain simulation result for the second proposed low-THz antenna (a) gain and (b) directivity

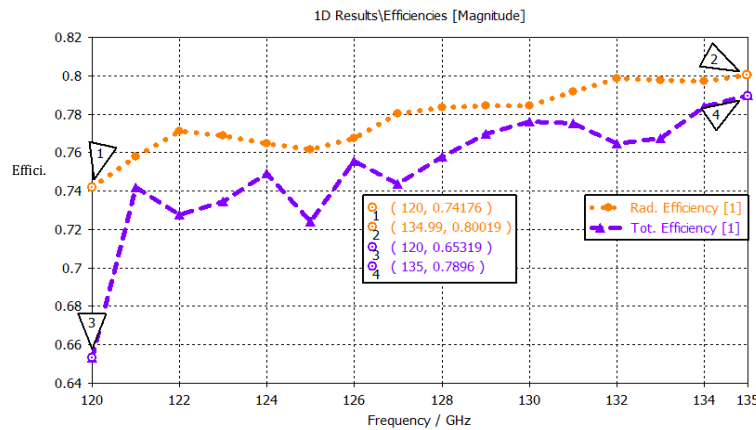


Figure 12. The radiation and the total efficiency simulated results of the second proposed low-THz antenna

3.4. Comparison of the first and second proposed low-THz antennas simulation results

The simulation results from comparing the S-parameters and gains of the first and second proposed THz antennas are shown in Figures 13(a) and 13(b). From Figure 13(a), it has been shown that the BW is lower by 0.18 GHz. This reduction happens when inserting the FSSs into the antenna. On the other hand, from Figure 13(b), it may have been shown that the antenna gain with FSSs was more considerable by 0.6 dB between the frequency of 124.7–128.4 GHz vs. without FSSs, and the peak change was 1.1 dB@124.75 GHz, i.e., inserting the FSSs is increasing the antenna gain at part of the THz frequency regime.

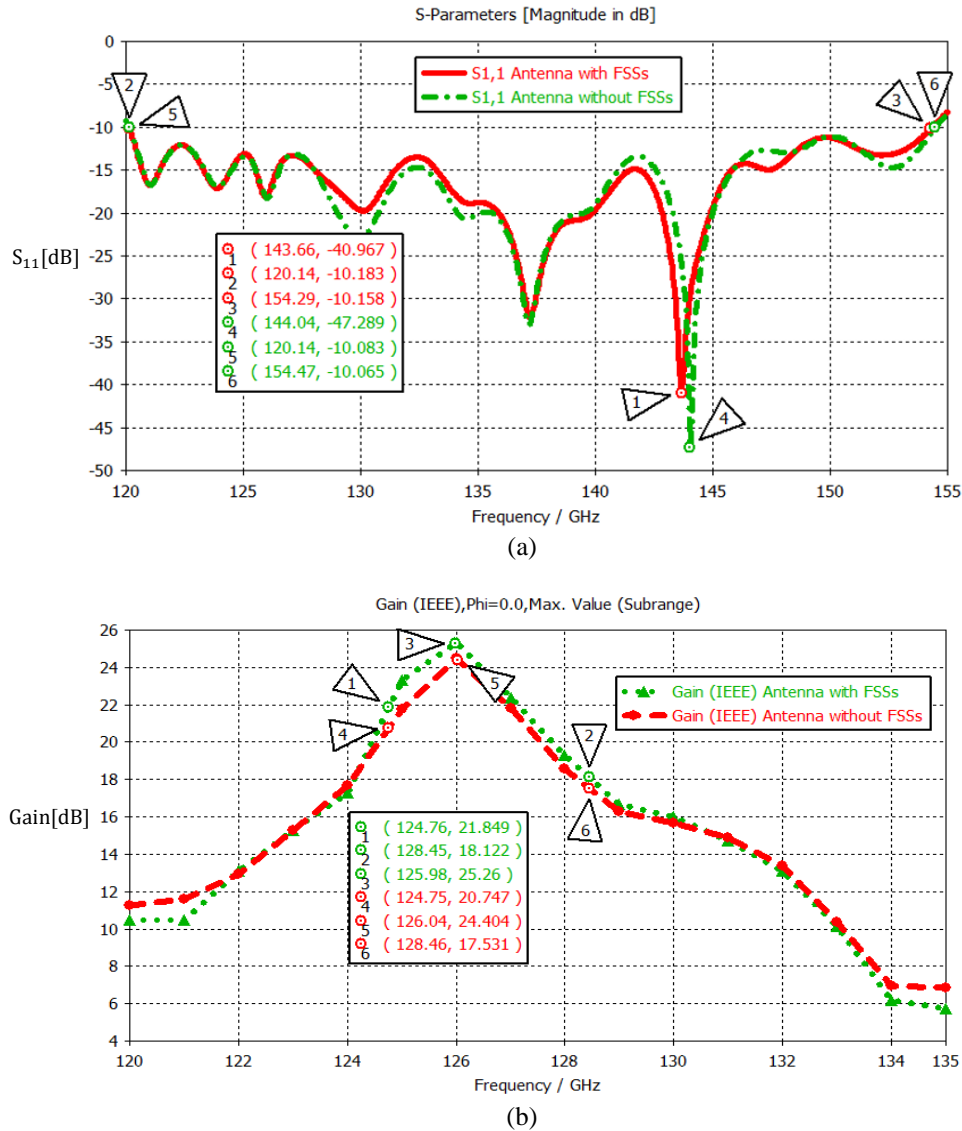


Figure 13. Simulation results from the comparison between the offered first and second low-THz antennas (a) simulation results of S_{11} and (b) simulation results of the gain

3.5. Comparison of the first proposed low-THz antenna simulation results

A comparison of the simulated results of the gain and S_{11} is shown in Figures 14(a) and 14(b), respectively. From Figure 14(a), it has been shown that the maximum obtained gain from the CST MWS software was 24.51 dB, while the maximum obtained gain from the Ansys HFSS software was 23.55 dB. In contrast, from Figure 14(b), it has been shown that the BW obtained from the CST MWS software was more than 19 GHz (121→140 GHz), while the BW obtained from the Ansys HFSS software was more than 19 GHz (121→140 GHz), so fair consent through the simulation results is obtained concerning the first proposed THz antenna by comparison with the Ansys HFSS and CST MWS software.

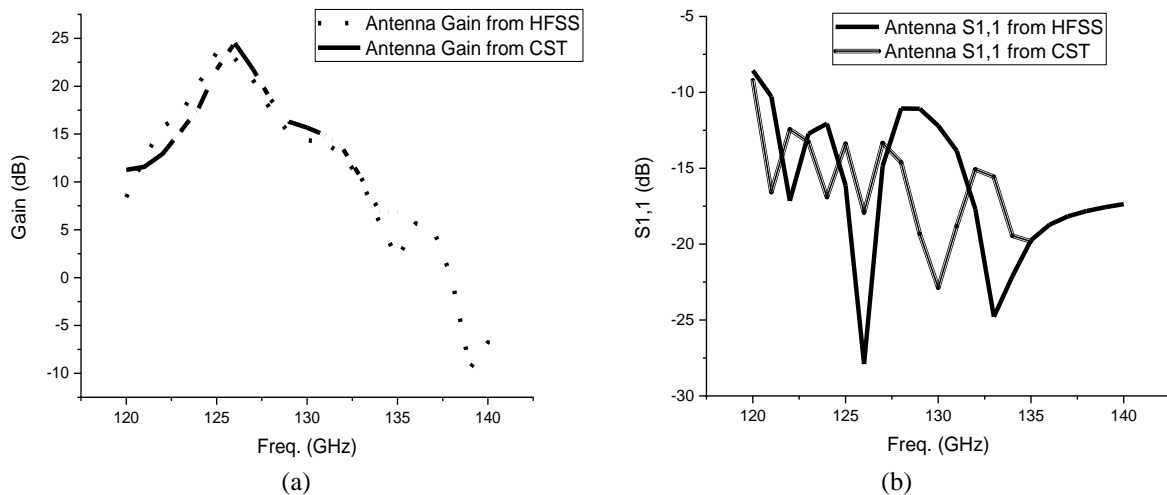


Figure 14. Comparison of the simulation results for the first proposed low-THz antenna (a) the comparison of the gain and (b) the comparison of S_{11}

4. DISCUSSION

High-directivity microstrip antennas are needed for 6G cellular communication at low THz to compensate for high losses in a humid atmosphere. However, according to [1], [3], and [22]–[28], the minimal gain for 144 GHz antennas enables the signal to propagate beyond 100 meters at least 16.85 dB, while BW facilitates a data rate of 20 Gb/s is 4.1 GHz. Therefore, this work aimed to model and simulate a microstrip array antenna at a frequency of 144 GHz with good BW and gain to maintain 6G cellular communication at the low-THz band and compared the simulation results with the Ansys HFSS software. At the first proposed low-THz antenna, the peak directivity, peak gain, peak radiation, total peak efficiency, and BW received were 25.6 dBi, 24.5 dB, 81.88%, 80.99%, and 34.39 GHz (25.04%), respectively. In contrast, at the second proposed THz antenna, the peak directivity, peak gain, peak radiation, total peak efficiency, and BW 27.01dBi, 25.3 dB, 80%, 78.96%, and 34.21 GHz (24.93%), respectively.

Choosing the suitable microstrip laminate becomes a critical challenge at Sub-mm and mm wavelengths because of laminate losses and conductor losses [17]–[19]. All PCBs have conduction losses and dielectric losses. And hence with these substrate parameters, which were ($h = 127 \mu\text{m} \leq \lambda_{\text{high}}/8 = 242 \mu\text{m}$), ($t = 17.5 \mu\text{m} \leq \lambda_{\text{high}}/8 = 242 \mu\text{m}$, $\epsilon_r = 2.2 < 3.5$, $\tan(\delta) = 0.0009 < 0.0095$) [17]–[19], the above effects were reduced to a minimum. The first proposed THz simulation results with the CST MWS software were compared with an Ansys HFSS software, and a fair agreement was obtained to cut down the cost of an empirical evaluation with a fabricated prototype low-THz antenna.

It may have been shown that this work's simulation results were compared with an Ansys HFSS software. Not similar to that obtained in work [9], where experimental measurements did verification. While at work [7]–[9], and [10], [11], the simulation results were neither validated nor compared. At this work, like work [9], the wanted THz antenna design was done with the CST MWS software, while at works [7], [8] and [10], the modeling and simulating of the wanted THz antenna were made with an Ansys HFSS software. The array and FSS structures have been used to increase the proposed design's directivity in this research, where at [9], [11], the lens techniques have been used to increase the antenna's directivities. In this research, a 1×32 power splitter was used to increase the antenna's directivities compared to [10], where a 1×2 power splitter was used. Unlike the works [7]–[11], in this work, we used the passband and stopband FSS structures to boost the antenna's directivity, while at work [7], the FSSs with stopband structures were used. This research attained the highest antenna directivity for the microstrip antenna than the works [7]–[11]. The slot patches have been used for expanding the BW of the proposed antenna design. At works [7] and [11], a non-conventional patch antenna has been used for the same purpose. This research attained the highest antenna BW for the microstrip antenna than the works [7]–[11], unlike works [9]–[11], where one antenna model was modeled and simulated. In contrast, a couple of antennas were modeled and simulated at this work, and the second antenna model had a larger directivity, like works [7], while at work [8], four THz antenna models were modeled and simulated. To sum up this discussion, the forthcoming Table 2 is attached. This table compares with other reported literature vs. this work in terms of technology, nominal frequency, BW, maximum directivity/maximum gain radiation, and total efficiency and verification/comparison method. It is observed from the data in Table 2 that the proposed antennas offer good characteristics in terms of gain

and total peak efficiency in comparison to [7]–[11], which makes them a candidate for 6G cellular communication antennas at low-THz.

Table 2. Comparison with other reported kinds of literature

Ref.	Antenna technology	Freq. nom. (GHz)	BW (GHz/%)	Max. directivity/gain (dBi/dB)	Max. radiation and total efficiency (%)	Verification/ Comparison
[7]	Rectangular patch	1000	16 GHz/1.6%	8.82 dB	n/a	No
	Bow-tie patch	1000	50 GHz/5%	12.92 dB	n/a	
[8]	Single rectangular	272	10 GHz/3.6%	7.5 dBi/1.6 dB	24	No
	Double rectangular stack	272	7 GHz/2.58%	7.8 dBi/2.4 dB	29	
	Double circular stack	272	10 GHz/3.6%	8.1 dBi/2.5 dB	30	
	Circular stack	272	11 GHz/4%	8.3 dBi /3.4 dB	32	
[9]	Dielectric lens	270	80 GHz/29.6%	30 dB	n/a	Experimental
[10]	1×2 array	1,000	210 GHz/21%	5.87 dBi	n/a	No
[11]	Quartz hemisphere lens	800	800/100%	13.2 dB	95/94.8	No
This work	26×32 slotting patch	144	34.39/25%	25.6 dBi/24.5 dB	81.88/80.99	Comparison
	26×32 slotting patch with stopband and passband FSSs	143.7	34.21/24.9%	27.01 dBi/25.3 dB	80/78.96	with Ansys HFSS

5. CONCLUSION

We modeled and simulated broadband low-THz microstrip array antennas with the CST MWS software at a resonance frequency of 144 GHz. These antennas have suitable gain and BW to support 6G communication at the low-THz band and compared the simulation results with Ansys HFSS software, supporting the proposed design. As a result, the peak directivity, peak gain, peak radiation, total peak efficiency, and BW obtained for the first and the second THz microstrip antennas without FSS and with FSS were 25.6 dBi, 24.5 dB, 81.88%, 80.99%, 34.39 GHz (25.04%), 27.01 dBi, 25.3 dB, 80%, 78.96%, and 34.21 GHz (24.93%), respectively. Thus, these antennas can be a base for 6G cellular communication at the low-THz regime. However, an empirical evaluation with a prototype fabricated low-THz antenna needs to be done to get more accurate validation.

REFERENCES

- [1] K. R. Jha and G. Singh, *Terahertz planar antennas for next generation communication*. Cham: Springer International Publishing, 2014, doi: 10.1007/978-3-319-02341-0.
- [2] K. Tekbilyk, A. R. Ekti, G. K. Kurt, and A. Görçin, “Terahertz band communication systems: challenges, novelties and standardization efforts,” *Physical Communication*, vol. 35, Aug. 2019, doi: 10.1016/j.phycom.2019.04.014.
- [3] I. F. Akyildiz, C. Han, and S. Nie, “Combating the distance problem in the millimeter wave and terahertz frequency bands,” *IEEE Communications Magazine*, vol. 56, no. 6, pp. 102–108, Jun. 2018, doi: 10.1109/MCOM.2018.1700928.
- [4] T. A. Nisamol, K. K. Ansha, and P. Abdulla, “Design of sub-THz beam scanning antenna using luneburg lens for 5G communications or beyond,” *Progress In Electromagnetics Research C*, vol. 99, pp. 179–191, 2020, doi: 10.2528/PIERC19121101.
- [5] K. Huang and Z. Wang, “Terahertz terabit wireless communication,” *IEEE Microwave Magazine*, vol. 12, no. 4, pp. 108–116, Jun. 2011, doi: 10.1109/MMM.2011.940596.
- [6] U. Nissanov and G. Singh, “Terahertz antenna for 5G cellular communication systems: a holistic review,” in *IEEE International Conference on Microwaves, Antennas, Communications and Electronic Systems (COMCAS)*, Nov. 2019, pp. 1–6, doi: 10.1109/COMCAS44984.2019.8958022.
- [7] M. Koutsoupidou, N. Uzunoglu, and I. S. Karanasiou, “Antennas on metamaterial substrates as emitting components for THz biomedical imaging,” in *IEEE 12th International Conference on Bioinformatics & Bioengineering (BIBE)*, Nov. 2012, pp. 319–322, doi: 10.1109/BIBE.2012.6399643.
- [8] B. Benakaprasad, A. Eblabla, X. Li, D. J. Wallis, I. Guiney, and K. Elgaid, “Design and performance comparison of various terahertz microstrip antennas on GaN-on-low resistivity silicon substrates for TMIC,” in *Asia-Pacific Microwave Conference (APMC)*, Dec. 2016, pp. 1–4, doi: 10.1109/APMC.2016.7931368.
- [9] K. Konstantinidis *et al.*, “Low-THz dielectric lens antenna with integrated waveguide feed,” *IEEE Transactions on Terahertz Science and Technology*, vol. 7, no. 5, pp. 572–581, Sep. 2017, doi: 10.1109/TTHZ.2017.2725487.
- [10] K. Tsugami, T. Asano, and H. Kanaya, “Wideband slot array antenna for 1 THz band imaging device,” in *IEEE 20th Electronics Packaging Technology Conference (EPTC)*, Dec. 2018, pp. 147–150, doi: 10.1109/EPTC.2018.8654353.
- [11] M. Faridani and M. Khatir, “Wideband hemispherical dielectric lens antenna with stable radiation pattern for advanced wideband terahertz communications,” *Optik*, vol. 168, pp. 355–359, Sep. 2018, doi: 10.1016/j.ijleo.2018.04.028.
- [12] U. Nissanov, G. Singh, E. Gelbart, and N. Kumar, “Highly directive microstrip array antenna with FSS for future generation cellular communication at THz band,” *Wireless Personal Communications*, vol. 118, no. 1, pp. 599–617, May 2021, doi: 10.1007/s11277-020-08034-2.
- [13] U. Nissanov, G. Singh, and N. Kumar, “High gain microstrip array antenna with SIW and FSS for beyond 5 G at THz band,” *Optik*, vol. 236, Jun. 2021, doi: 10.1016/j.ijleo.2021.166568.
- [14] SIMULIA, “CST studio suite electromagnetic field simulation software,” *Dassault Systèmes*, <https://www.3ds.com/products-services/simulia/products/cst-studio-suite> (accessed Jun. 1, 2021).
- [15] Ansys, “Ansys HFSS best-in-class 3D high frequency electromagnetic simulation software,” *Ansys*, <https://www.ansys.com/products/electronics/ansys-hfss> (accessed Jun. 1, 2021).

- [16] Z.-W. Miao, Z.-C. Hao, Y. Wang, B.-B. Jin, J.-B. Wu, and W. Hong, "A 400-GHz high-gain quartz-based single layered folded reflectarray antenna for terahertz applications," *IEEE Transactions on Terahertz Science and Technology*, vol. 9, no. 1, pp. 78–88, Jan. 2019, doi: 10.1109/TTHZ.2018.2883215.
- [17] J. du Preez and S. Sinha, *Millimeter-wave antennas: configurations and applications*. Springer International Publishing, 2016, doi: 10.1007/978-3-319-35068-4.
- [18] G. Kouemou, *Radar Technology*, InTech, 2010, doi: 10.5772/130.
- [19] L. K. S. Granados, "Antennas for millimeter-Wave Applications," Instituto Nacional de Astrofísica, Óptica y Electrónica (INAOE).
- [20] C. A. Balanis, *Antenna theory: analysis and design*. John Wiley & Sons, 2015.
- [21] F. Capolino, *Theory and phenomena of metamaterials*. CRC Press, 2017, doi: 10.1201/9781420054262.
- [22] T. Kleine-Ostmann and T. Nagatsuma, "A review on terahertz communications research," *Journal of Infrared, Millimeter, and Terahertz Waves*, vol. 32, no. 2, pp. 143–171, Feb. 2011, doi: 10.1007/s10762-010-9758-1.
- [23] K. R. Jha and G. Singh, "Terahertz planar antennas for future wireless communication: a technical review," *Infrared Physics and Technology*, vol. 60, pp. 71–80, Sep. 2013, doi: 10.1016/j.infrared.2013.03.009.
- [24] M. Tamagnone, J. S. Gómez-Díaz, J. R. Mosig, and J. Perruisseau-Carrier, "Analysis and design of terahertz antennas based on plasmonic resonant graphene sheets," *Journal of Applied Physics*, vol. 112, no. 11, Dec. 2012, doi: 10.1063/1.4768840.
- [25] V. Petrov, A. Pyattaev, D. Moltchanov, and Y. Koucheryavy, "Terahertz band communications: applications, research challenges, and standardization activities," in *8th International Congress on Ultra Modern Telecommunications and Control Systems and Workshops (ICUMT)*, Oct. 2016, pp. 183–190, doi: 10.1109/ICUMT.2016.7765354.
- [26] T. Kürner and S. Priebe, "Towards THz communications - status in research, standardization and regulation," *Journal of Infrared, Millimeter, and Terahertz Waves*, vol. 35, no. 1, pp. 53–62, Jan. 2014, doi: 10.1007/s10762-013-0014-3.
- [27] T. T. Ha, *Theory and design of digital communication systems*. Cambridge University Press, 2010, doi: 10.1017/cbo9780511778681.
- [28] U. Nissanov, G. Singh, P. Kumar, and N. Kumar, "High gain terahertz microstrip array antenna for future generation cellular communication," in *International Conference on Artificial Intelligence, Big Data, Computing and Data Communication Systems (IABCD)*, Aug. 2020, pp. 1–6, doi: 10.1109/icABCD49160.2020.9183864.

BIOGRAPHY OF AUTHORS



Uri Nissanov (Nissan)    completed a Ph.D. in Electrical and Electronic Engineering with Excellence at the University of Johannesburg, South Africa, in 2022, where his thesis was to analyze and design a Terahertz (THz) microstrip antenna for next-generation communication systems. In addition, he holds M.Sc with a thesis and B.Tech. in Electric and Electronic Engineering with Excellence, all from of University of Ariel, Israel. Besides that, he holds an M.Sc in Electric and Electronic Engineering with Excellence from Holon Institute of Technology (HIT), Israel. In addition, now he is doing post-Doctoral fellow research at the University of Johannesburg, South Africa, on antenna technology for THz wireless communication. His research interests are in the design and simulation of THz band/sub-mmWave/mmWave high-gain, broadband microstrip array antennas, reconfigurable antennas, beam steering microstrip antennas, and components such as Wilkinson power dividers, T-power dividers, frequency selective surfaces (FSSs), substrate integrated waveguides (SIWs) and beam-steering Rotman Lens. He can be contacted at email: uri1636@gmail.com.



Ghanshyam Singh    received a Ph.D. degree in Electronics Engineering from the Indian Institute of Technology, Banaras Hindu University, Varanasi, India, in 2000. He was associated with the Central Electronics Engineering Research Institute, Pilani, and Institute for Plasma Research, Gandhinagar, India. He was a research scientist and worked as an Assistant Professor at the Electronics and Communication Engineering Department at Nirma University of Science and Technology, Ahmedabad, India. He was a Visiting Researcher at the Seoul National University, Seoul, South Korea. He also worked as an Assistant Professor, Associate Professor, and Full Professor in the Department of Electronics and Communication Engineering at the Jaypee University of Information Technology, Solan, India. He is a Full Professor with the Department of Electrical and Electronics Engineering, APK Campus, University of Johannesburg, S Africa. He is an author/co-author of more than 250 scientific papers in the refereed Journal and International Conferences. His research and teaching interests include RF/Microwave Engineering, Millimeter/THz Wave Antennas and their Applications in Communication and Imaging, Next-Generation Communication Systems (OFDM and Cognitive Radio), and Nanophotonic. He has more than 19 years of teaching and research experience in electromagnetic/microwave engineering, wireless communication, and nanophotonic. He has supervised 15 Ph. D. and 45 M. Tech. Theses. He has worked as a reviewer for several reputed Journals and Conferences. He is the author of four books published by Springer. He can be contacted at email: ghanshyams@uj.ac.za.